J. Environ Science & Engg., Vol. 57, No. 3, P 203-213, July 2015

Rapid and Green Synthesis of Gold Nanoparticles by the Use of an Otherwise Worthless Weed lantana (*Lantana camara* L.)

J. ANURADHA[1], TASNEEM ABBASI[2] AND S. A. ABBASI[3]*

The phyto-fabrication of gold nanoparticles utilizing the highly invasive terrestrial weed, *Lantana camara,* is presented. In an attempt to utilize the entire plant, the extracts of all its parts – leaves, stem and root – were employed in various proportions with the gold precursor, $HAuCl_4$ solution, for the synthesis. The reduction of gold ions to nanoparticles was tracked using UV-Vis spectroscopy. The electron micrographs of the synthesized nanoparticles revealed the presence of particles of monodispersed spherical and polydispersed triangular, pentagonal, rod and truncated triangular shapes in sizes ranging 15–55 nm and 7–100 nm respectively. The presence of gold atoms was confirmed from the EDAX and X-Ray diffraction studies. The FT–IR spectral study indicated that the alkanes in the plant extract could have been responsible for the reduction of the gold ions to gold nanoparticles.

Key words: *Phyto-fabrication, Lantana camara, gold nanoparticles, monodispersed particles, TEM*

1.0 Introduction

Gold nanoparticles (GNPs) find wide application due to their special catalytic, optical, biosensor, magnetic and electrical properties[1-4], and their use has led to the opening of new avenues in nanoimmunology, nanomedicine, and nanobiotechnology[5]. This is due to the properties of GNPs which very subtly with their sizes and shapes. Hence synthesis of different forms of GNPs in an economical and eco-friendly manner forms an important thrust area of nanotechnology.

Among the available means for GNPs synthesis, the physical and chemical methods often require high temperatures/ pressures, and/or high energy inputs, and involve hazardous chemicals either as reducing agents and/or as stabilizing agents for the nanoparticles (NPs) formation. The physical conditions required for NPs generation is highly intensive and expensive; and the use of toxic chemicals in the synthesis process releases hazardous byproduct that may affect the environment in addition to human health. Consequently, the bioinspired GNP synthesis is gaining importance not only due to its low cost and high reproducibility, but also its eco-friendliness. Recently there have been numerous reports on extra-cellular Au NPs synthesis using living organisms such as actinomycetes, bacteria, fungi, algae, and/or vascular plant extracts. Of these the phyto-fabrication of NPs is beneficial over the other bioagents because it is rapid and convenient. It is not constrained by the need for elaborate and fine maintenance that characterize microorganism-base NP synthesis method. These are also free from the risk of microbial contamination; and are easy to be scaled up for large scale NPs synthesis[6-10].

Several plant species have been explored for their potential to generate nanoparticles when the plant extracts are combined with Au (III) solutions. However most of these studies have employed species encompassing fruits, vegetables, cereals, spices, medicinals and other foodstuff, which already have well-established uses and entail substantial costs of production[11, 6, 8, 12, 10]. Some of the attempts that have been made in the past to utilize lantana in the synthesis of silver[12, 13-15] and copper nanoparticles[16] but there is no report on the possible use of the weed in the manufacture of GNPs. In the present work, we have

[1]PhD Research Scholar, [2]Assistant Professor, [3]Professor,
Centre for Pollution Control and Environmental Engineering, Pondicherry University, Puducherry - 605 014.
*Corresponding author:prof.s.a.abbasi@gmail.com

developed method which employs invasive plant species lantana (*Lantana camara*) for GNPs synthesis. As this plant has no pre-existing commercial value, rather it consumes resources for keeping them in check; this approach is doubly beneficial: it helps the cause of environmental protection as well as to improve the economics of nanoparticle synthesis. Moreover in the past all authors have used – mainly the leaves – of the different plants for GNPs synthesis. In contrast the present investigation is based on the use of whole plant of the highly pernicious invasive weed *Lantana camara* (L.). This is a very significant improvement because on one hand it enhances the utility value of each plant manifold and on the other hand it makes the utilization of the invasives so potentially gainful that it may become remunerative to control the invasives through their harvesting and use.

Lantana (*L. camara*) is an erect shrub, belonging to the Verbenaceae family. It is very hardly, resilient and productive. These attributes have made lantana one of the most powerful of all invasive plants. It is regarded as one among the world's top ten noxious weeds. Its distribution encompasses over sixty countries in the tropical and subtropical world, covering millions of hectares of land.

Due to its resistance to all attempts at eradication, the plant invades natural communities by monopolizing the available light, water, nutrients and space. As a result, the ecosystem structure and function alters due to the cumulative consequence of reduction in species diversity and richness of native vegetation[17-19]. Its allelopathic properties further bolster its invasiveness[12].

1.2 Experimental

1.2.1 Preparation of aqueous extracts of the leaf, stem and root of lantana

L. camara was collected from its natural habitat near Pondicherry (central) University, Puducherry. The fresh, mature, and disease-free plant portions were washed thoroughly with water, then dipped in saline water to sterilize their surface, followed by washing them liberally before blotting them dry. A known quantity of plant samples was dried at 105°C to a constant weight[20]. On the basis of dry weight thus obtained, extracts for nanoparticle synthesis were made by boiling 1.0 g of the plant material with 100 mL of sterile distilled water for 5 minutes. The contents were filtered through a Whatmann No. 42 filter paper and the filtrates were stored under refrigeration at 4°C[7, 21, 8, 12]. Reconnoitery experiments revealed that the extracts retained their integrity till a little more than 3 days as indicated by the extent of nanoparticles generated by them. Hence in all the experiments the extracts were used only till 3 days after preparation.

1.2.2 Au (III) solution

A 10^{-3} M aqueous solution of *Au (III)* was prepared using analytical reagent grade $HAuCl_4$. The stock solution was stored in amber bottles covered with black sheets.

1.2.3 Nanoparticle synthesis

The plant extracts were mixed with *Au (III)* solution at ambient temperature. The gold nanoparticles (GNPs) began forming almost immediately as indicated

Table 1: Extract and metal solution combinations studied for gold nanoparticles synthesis using *L. camara*

Plant used	Plant part used for preparing the extract	Concentration of component in the reaction mixture (mg/ L)	
		Extract	Au (III)
L. camara	Leaf (LE_1)	7000	100
	Leaf (LE_2)	4650	30
	Stem (SE_1)	4650	110
	Stem (SE_2)	4650	70
	Root (RE_1)	2000	110
	Root (RE_2)	4650	70

by the appearance of pinkish red or purple colour which grew in intensity with time. The developed colour and its intensity depended on the stoichiometric ratio in which the plant extract and the metal ion had been mixed. The spectra of the reaction mixtures were recorded using UV-visible spectrophotometer. In a typical experiment for green synthesis of gold nanoparticles, the plant extracts of *L. camara*, were mixed with Au (III) solution in the proportion as presented in Table 1.

1.2.4 Characterization of the synthesized gold nanoparticles

1.2.4.1 UV-Visible spectroscopy

UV–visible (UV-vis) spectroscopy is an essential means to track the synthesis of the aqueous metal nanoparticles. The bioreduction of the gold ions was monitored by recording the UV–vis spectra in the range of 190–1100 nm for the reaction mixture filled in quartz cuvettes with 1 cm path length at our laboratory. De-ionized distilled water was used as blank. The spectral observation of the reaction mixtures was recorded by employing Labindia (model UV 3000+) and ELICO (model SL 164) double beam UV–visible spectrophotometers operated at 1 nm resolution.

1.2.4.2 SEM/TEM studies

SEM (Scanning electron microscopy) and TEM (Transmission electron microscopy) studies were carried out to determine the size and morphology of the synthesized gold nanoparticles. The synthesized gold nanoparticles present in the extract and unreduced metal ion solution mixture were centrifuged at 12,000 rpm for 20 minutes using Remi C 24 centrifuge. The resulting pellets were washed thrice with de-ionized distilled water to remove the unreacted constituents and were re-dispersed in de-ionized distilled water.

The samples for SEM studies were prepared by placing a drop of suspension on a carbon-coated SEM grid. The micrographs were recorded by employing a scanning electron microscope (SEM). For high resolution scanning electron microscopic studies the samples were prepared by placing dried pellets on a carbon coated aluminium stub. The nanoparticles were prepared for TEM studies by first pelletizing the nanoparticles by diluting and through sonication. The micrographs were recorded by depositing a drop of the well dispersed samples on carbon coated 300 mesh placed on copper TEM grids and excess liquid was wiped off with filter paper.

1.2.4.3 Energy dispersive X-ray (EDAX) studies

The identification of the elemental composition of the synthesized nanoparticles was performed using the EDAX equipment attached with the SEM/HRSEM microscopes. The EDX spectrum was recorded after documenting the electron micrographs in the spot-profile mode by focusing on the densely occupied gold nanoparticle region.

1.2.4.4 Selected area electron diffraction (SAED) studies

The SAED pattern recorder was equipped with TEM instrument; hence the SAED patterns were documented along with the TEM micrographs.

1.2.4.5 X-ray diffraction (XRD) studies

The powder XRD (X-Ray Diffraction) spectrum of the NPs was recorded to investigate the crystallinity of the material being analyzed. An aliquot of the pelletized gold nanoparticles was drop-casted to thin film on a glass slide and the spectral recording was executed by scanning in the 2è region, from 0° to 80°, at 0.02° per minute, and with the time constant of 2 seconds. The crystalline pattern of the nanoparticles was recorded using Cu $K_{\alpha 1}$ radiation with a wavelength (ë) of 1.5406Å at a tube voltage of 40 kV and a tube current of 30 mA.

1.2.4.6 Fourier transform infrared spectroscopic (FTIR) studies

FT-IR spectroscopy was used to help identify the functional groups involved in the reduction, stabilization and capping of the gold nanoparticles. For performing the FT-IR studies, the samples were dried completely and ground with potassium bromide. The spectrum was recorded at diffuse reflectance mode with 4 cm^{-1} resolution in the mid-IR region between the Wavenumbers 4000 and 400 cm^{-1}.

1.3 Results and discussion

1.3.1 UV–visible spectra

The commencement of the gold nanoparticle formation was observed from the gradual appearance of pinkish red and violet color within 10 minutes of mixing the metallic solution with the plant extract. This change in colour is attributable to the localized surface plasmon resonance (SPR); which is the collective vibration of free conduction electrons induced by an interacting electromagnetic field of the gold nanoparticles[22].

Table 2 : Summary of results obtained from the UV-visible spectral studies for gold nanoparticles synthesized using *L. camara* extracts

Extract + Metal ion mixture		LE_1	LE_2		SE_1	SE_2	RE_1	RE_2	
0th h	λ_{max}	-	-	-	-	-		-	
	Abs.								
2nd h	λ_{max}	557					*590*		
	Abs.	1.760					*0.457*		
4th h	λ_{max}	540	542	1061			588	1056	
	Abs.	1.827	0.961	0.968			0.451	0.714	
6th h	λ_{max}	540	*540*	*1011*	568	1018	590	1045	
	Abs.	1.861	*1.138*	*1.085*	0.338	0.114	0.441	1.009	
24th h	λ_{max}	541	539	964	554	1042	590	1050	
	Abs.	1.912	1.278	1.166	0.510	0.745	0.421	1.216	
48th h	λ_{max}	540	538	958	551	1049	583	*1051*	
	Abs.	1.914	1.322	1.199	0.568	0.821	0.411	*1.250*	
72nd h	λ_{max}	*543*	539	955	548	995	-	1051	
	Abs.	*2.108*	1.383	1.232	0.653	0.850		1.246	
96th h	λ_{max}	542	-		*547*	*1049*		1051	
	Abs.	1.987			*0.730*	*0.843*		1.247	
120th h	-				550	1056			-
					0.697	0.872			
144th h					550	1056			
					0.615	0.879			
168th h					551	-			
					0.635				

The UV-vis spectral pattern observed was determined by the plant part used for preparing the extract and its proportions with respect to the metal solution. Two types of spectra were observed – one with a single λ_{max} in the visible region, and the other with two λ_{max}'s; one in the visible region and the other in the NIR (near infra-red) region. The reaction combinations LE_1, SE_1 and RE_1 (Fig. 1, 3 and 5) exhibited the single λ_{max} type of spectra while the LE_2, SE_2 and RE_2 (Fig. 2, 4 and 6) combinations exhibited the double λ_{max}–spectra. The presence of a single SPR peak in the visible region in the spectra of LE_1, SE_1 and RE_1 reaction combinations gave a hint that the synthesized GNPs were spherical; this was later confirmed from the recorded electron micrographs. The spectral pattern of LE_2, SE_2 and RE_2 combinations showed the presence of two prominent absorption bands– a shorter wavelength transverse absorption band in the visible region (out-of-plane vibration band) and a longer wavelength longitudinal absorption band in the NIR region (in-plane plasmon vibrations) – indicating anisotropic gold nanoparticle formation[23-25]. This observation was also confirmed from the electron microscopic studies.

The peak wavelengths (λ_{max}) observed from the UV-vis spectral studies are summarized in Table 2 for all the reaction combinations. To an extent, the intensity of the gold nanoparticle formation was found

Table 3 : 2θ position of the Bragg's plane observed from the X-ray diffractograms.

Bragg's plane		(111)	(200)	(220)	(311)
2θ position	LE_1	38.14	44.46	64.71	77.76
	LE_2	38.16	44.44	64.76	77.68
	SE_1	38.36	44.45	64.83	77.77
	SE_2	38.26	43.97	64.83	77.81
	RE_1	38.06	44.42	64.68	77.74
	RE_2	38.17	44.40	64.86	77.63

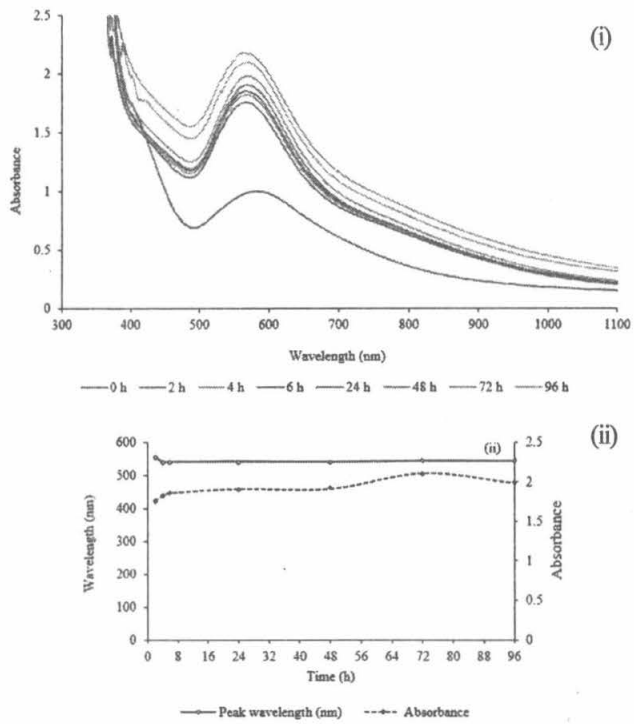

Fig. 1: UV-visible spectra of (i) LE_1 gold nanoparticles synthesis; (ii) Plot of the intensity of the surface plasmon resonances of LE_1 against the reaction duration

to rise up consistently with increase in the reaction duration.

The rate of nanoparticles formation was found to be completed within 6th, 72nd h for the leaf extracts (LE_1, LE_2), 96th h for the stem extracts (SE_1, SE_2), and

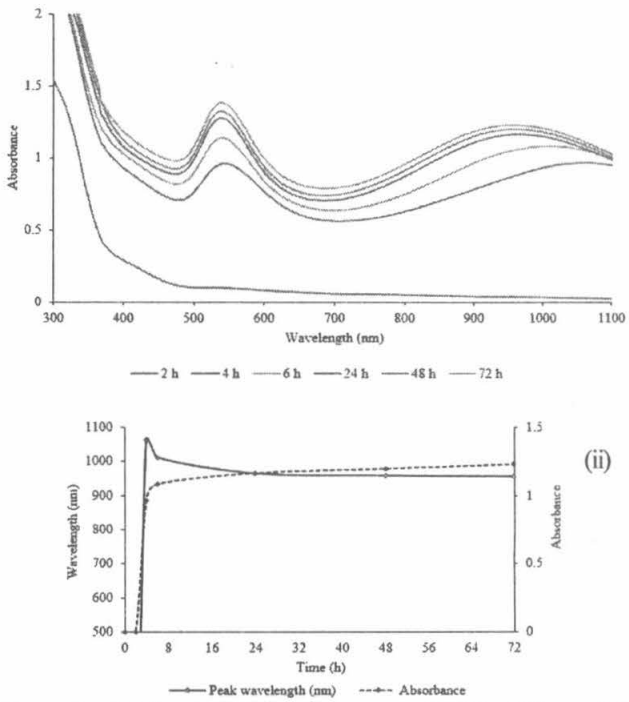

Fig. 2: UV-visible spectra of (i) LE_2 gold nanoparticles synthesis; (ii) Plot of the intensity of the surface plasmon resonances of LE_2 against the reaction duration

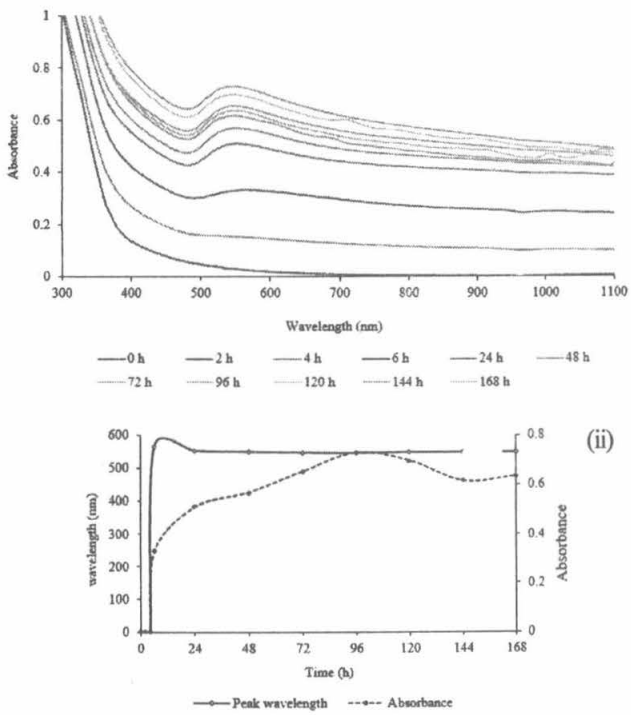

Fig. 3: UV-visible spectra of (i) SE_1 gold nanoparticles synthesis; (ii) Plot of the intensity of the surface plasmon resonances of PE_1 against the reaction duration

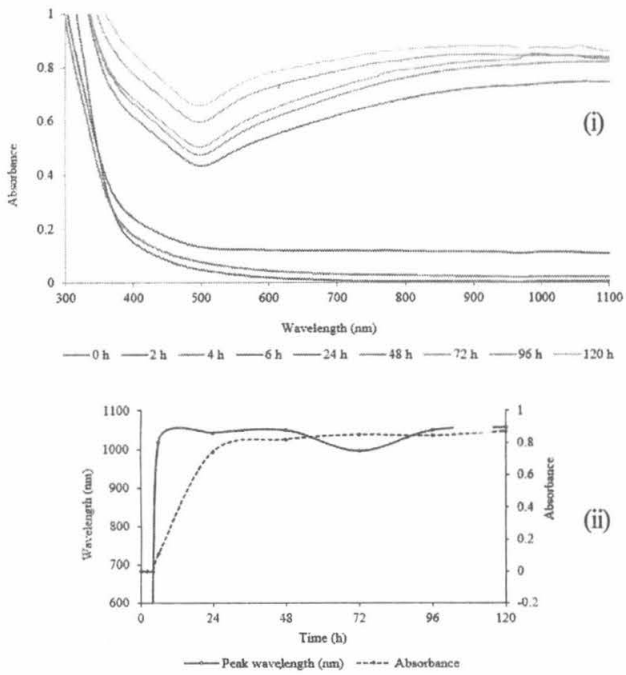

Fig. 4: UV-visible spectra of (i) SE_2 gold nanoparticles synthesis; (ii) Plot of the intensity of the surface plasmon resonances of PE_2 against the reaction duration

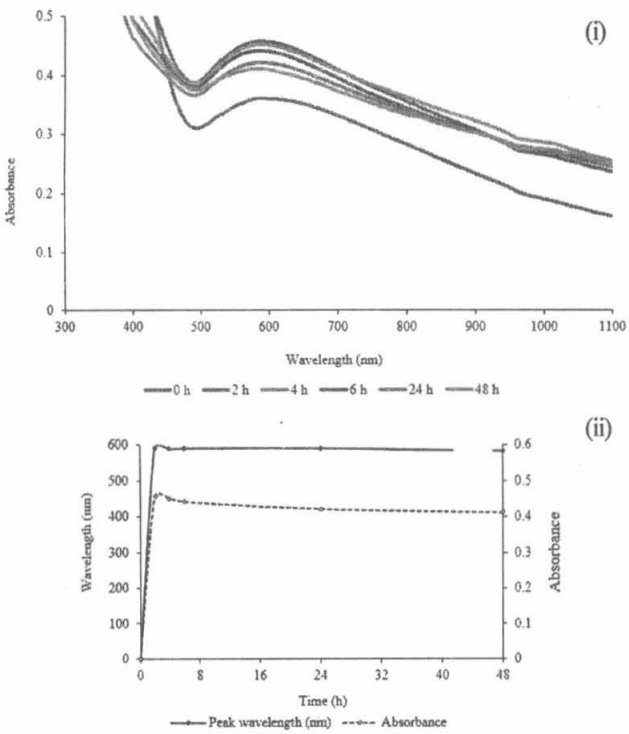

Fig. 5: UV-visible spectra of (i) RE_1 gold nanoparticles synthesis; (ii) Plot of the intensity of the surface plasmon resonances of RE_1 against the reaction duration

48th, 2nd h for root extracts (RE_1, RE_2) of the reaction duration.

The features of the synthesized GNPs were studied using SEM, Hr-SEM, TEM, EDX, XRD and SAED techniques and FT-IR spectroscopy was employed for identifying the biomolecules that could have possibly involved in the nanoparticles formation.

1.3.2 Electron microscopic (SEM, Hr-SEM, TEM) and EDX studies

The SEM and Hr-SEM images recorded for the nanoparticles synthesized from the LE_1, SE_1 and RE_1 combinations show that the nanoparticles are spherical in shape. The TEM micrographs of the GNPs show that the size of the synthesized particles ranges from of 16–27 nm, 15–45 nm, and 20–55 nm respectively for the LE_1, SE_1 and RE_1 combinations (Fig. 7, 9 and 11).

The electron microscopic studies (SEM, Hr-SEM and TEM) of the nanoparticles formed from the LE_2, SE_2 and RE_2 combinations are presented in Fig. 8, 10 and 12. It is seen that these reaction combinations resulted in anisotropic nanoparticles of triangular, pentagonal, rod and truncated triangular shapes. The sizes of the nanoparticles ranged from 20–100 nm, 25–80 nm, and 7–85 nm respectively for the reaction combinations LE_2, SE_2 and RE_2.

The spot-profile EDX spectrum shows a strong signal for gold atoms in the nanoparticles (Insets of Fig. 7–12). Weak signals from C, N and O atoms are also observed which are likely to be due to X-ray emission from the biomolecules like proteins/enzymes found in the residual plant extracts present along with the nanoparticles. An optical absorption peak at approximately 2 keV is seen, which is characteristic of gold nanoparticles[7, 8].

The SAED patterns are shown in Figures 7 (f) – 12 (f). The bright circular spots complement the Bragg's planes, confirming the crystalline nature of the gold nanoparticles[26].

1.3.3 X-ray diffraction (XRD) studies

The diffractograms (Fig. 13) have intense peaks at the 2θ position, corresponding to (111), (200), (220) and (311) Bragg's planes and indicating a face centered cubic structure of nanoparticles[27] (Table 3). The XRD patterns which match with the database of JCPDS file no. 04-0784, confirm that the synthesized

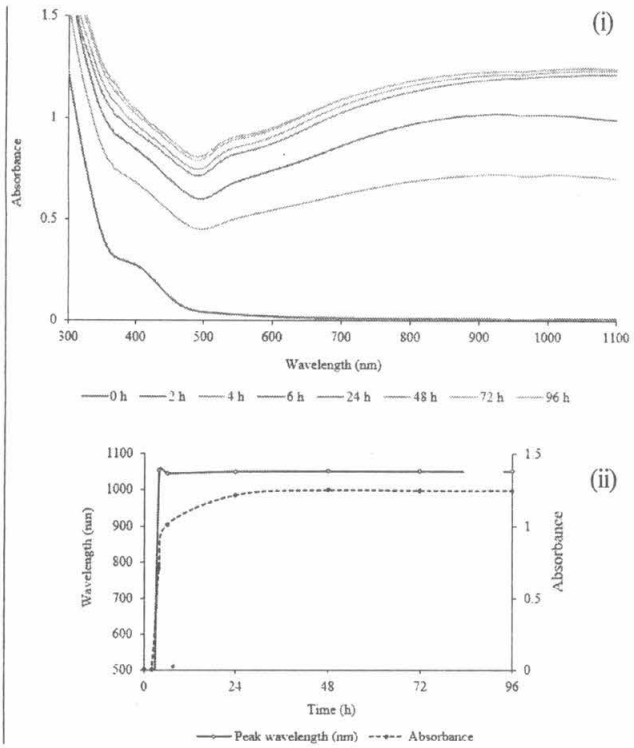

Fig. 6: UV-visible spectra of (i) RE_2 gold nanoparticles synthesis; (ii) Plot of the intensity of the surface plasmon resonances of RE_2 against the reaction duration

gold nanoparticles are of pure crystalline nature. The widening of Bragg's peak also confirms the nanoparticles formation. The crystalline domain size of the nanoparticles was calculated using the Debye–Scherrer's equation by obtaining the FWHM of the (111) Bragg's reflection from the XRD spectrum[28].

The crystalline sizes of the GNPs were found to be from 12.85 to 51.27 nm. The particle sizes determined from diffractograms (Fig. 13 a, c and e) are in agreement with the average size *ca.* 37.49 nm from the electron micrographs. This reveals the formation of monodispersed spherical particles. The particle size calculated from XRD pattern (Fig. 13 b, d and f) is less than that of the size determined from the electron micrographs. This is probably because the synthesized gold nanoparticles are of polycrystalline nature[29]. The ratio of optical density between the (200) and (111) Bragg's diffraction peaks is in the range of 0.13–0.35. This is found to be lesser than the intensity ratio (i.e. 0.52) of conventional bulk gold, indicating the presence of nanoparticles with (111) facets[30].

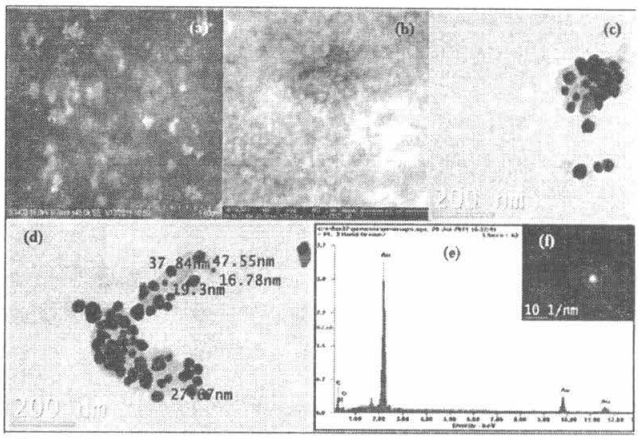

Fig. 7: Each visual is a composite of (a) SEM; (b) Hr-SEM; (c) & (d) TEM; (e) EDX spectrum (Inset is the (f) SAED pattern) of LE_1 gold nanoparticles

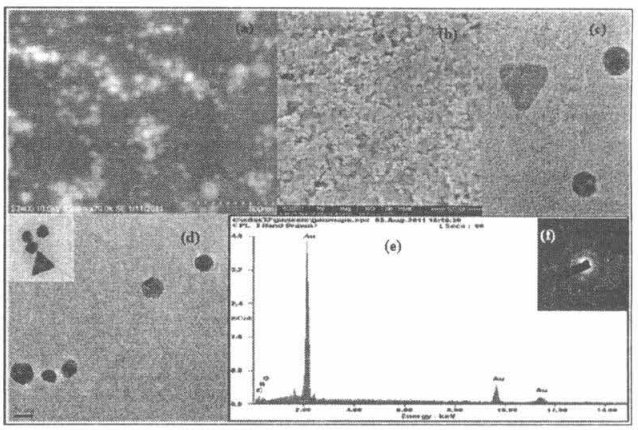

Fig. 8: Each visual is a composite of (a) SEM; (b) Hr-SEM; (c) & (d) TEM; (e) EDX spectrum (Inset is the (f) SAED pattern) of LE_2gold nanoparticles

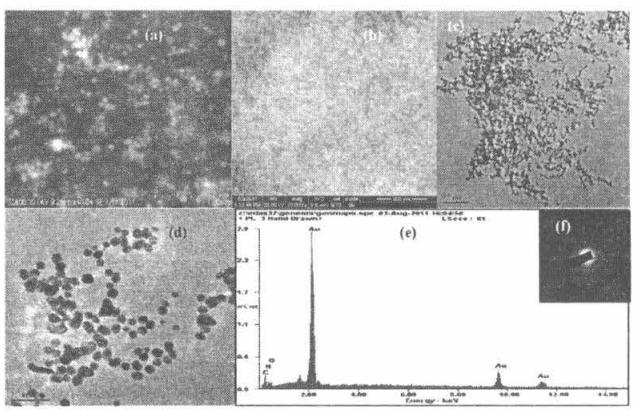

Fig. 9: Each visual is a composite of (a) SEM; (b) Hr-SEM; (c) & (d) TEM; (e) EDX spectrum (Inset is the (f) SAED pattern) of SE_1 gold nanoparticles

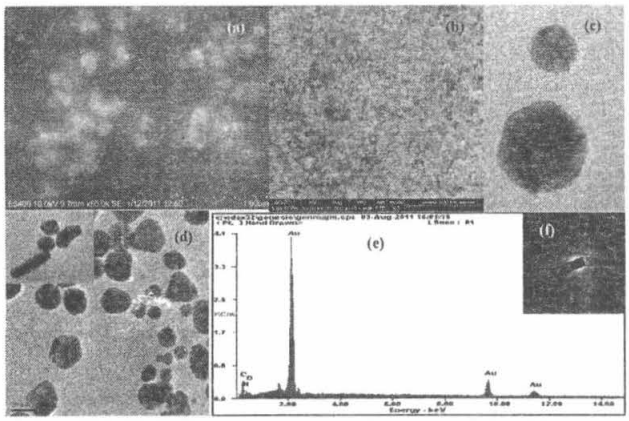

Fig. 10: Each visual is a composite of (a) SEM; (b) Hr-SEM; (c) & (d) TEM; (e) EDX spectrum (Inset is the (f) SAED pattern) of SE_2 gold nanoparticles.

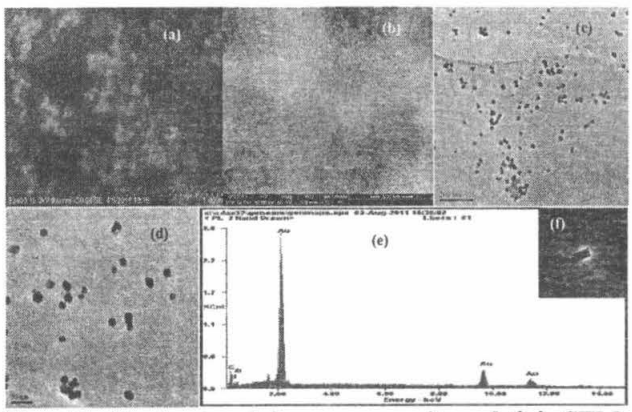

Fig. 11: Each visual is a composite of (a) SEM; (b) Hr-SEM; (c) & (d) TEM; (e) EDX spectrum (Inset is the (f) SAED pattern) of RE_1 gold nanoparticles

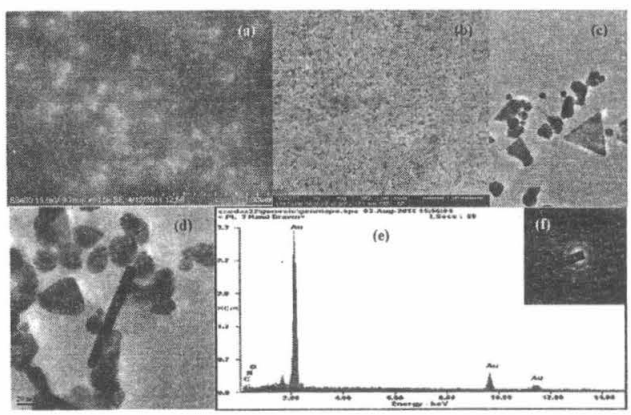

Fig. 12: Each visual is a composite of (a) SEM; (b) Hr-SEM; (c) & (d) TEM; (e) EDX spectrum (Inset is the (f) SAED pattern) of RE_2 gold nanoparticles

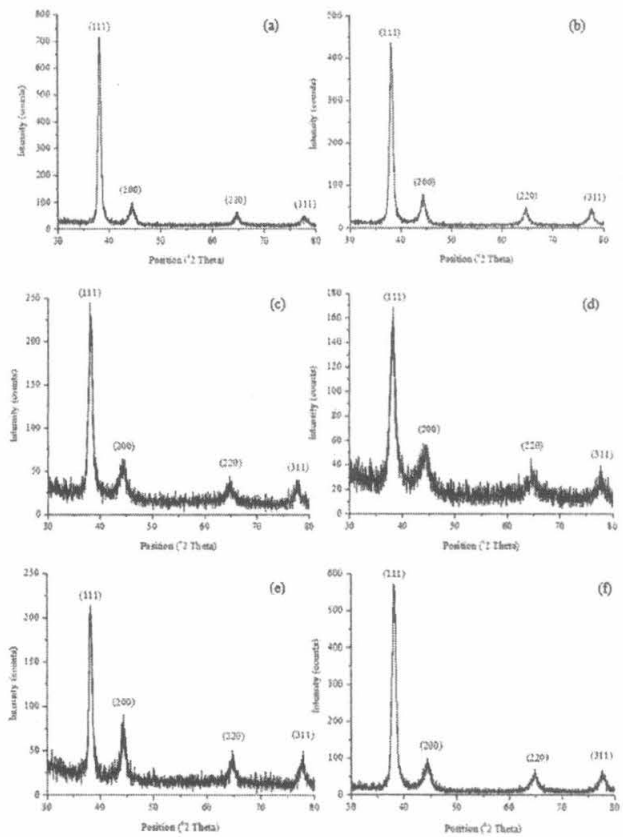

Fig. 13: X-ray diffraction spectrum of (a) LE_1, (b) LE_2, (c) SE_1, (d) SE_2, (e) RE_1 and (f) RE_2 gold nanoparticles

1.3.4 Fourier Transform infra-red (FT-IR) spectroscopy

FT–IR analysis was employed to identify the functional group of the biomolecules found in the plant extract which could have been involved in the bioreduction and capping/stabilization of the synthesized nanoparticles. The FT-IR spectra (Fig. 14) was able to show that amides, proteins and alkanes were possibly involved in the bioreduction and capping/ stabilization of the synthesized nanoparticles.

The FT–IR pattern of leaf extract showed the presence of medium or strong absorption bands at 1606 cm^{-1}, 1413 cm^{-1}, 1079 cm^{-1}. The strongest bands can be assigned to amide I[31-33]. The peak was found to shift to 1663 cm^{-1} and a peak at 1967 cm^{-1} appears in the spectra from the gold nanoparticles. This shows that amides found in the leaf extract could be responsible for the reduction of the gold ions and also acts as an efficient capping agent ensuring the stability of the phyto-fabricated nanoparticles.

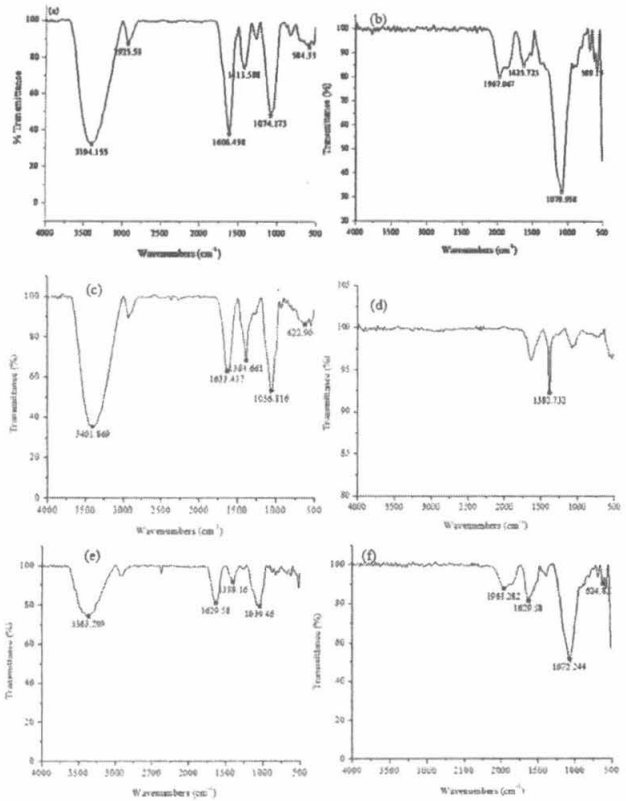

Fig. 14: The FTIR spectrum of *L. camara* (a) leaf, (c) stem, (e) root extracts and the synthesized gold nanoparticles (b, d and f) respectively

The peaks observed from the spectral pattern of stem extract were found at 1633 cm^{-1}, 1384 cm^{-1}, and 1052 cm^{-1}. In this case, too, the strongest band can be attributed to amines[31, 32]. Bands corresponding to amines and proteins at 1052 cm^{-1} were found to be shifted in the spectra from the gold nanoparticles. The peak at 1382 cm^{-1} corresponding to alkanes due to CH_3 band appears in the spectra from the gold nanoparticles. This indicates that proteins, alkanes found in the stem extract could have interacted in the bioreduction and capping/stabilization of synthesized gold nanoparticles.

The recorded spectral patterns of the root extract were found with the bands at 1629 cm^{-1}, 1398 cm^{-1}, 1039 cm^{-1} and the strongest band can be assigned to amide I[31-33]. On comparing the spectra of root extract and gold nanoparticles, Fig. 14 reveals the presence of minor changes in the positions as well as on the magnitude of the absorption bands. With closer examination, the spectrum of gold nanoparticles shows a minor shift to 1072 cm^{-1} and disappearance of band at 1398 cm^{-1}. The band at 1072 cm^{-1} corresponds to the alkanes. Hence, it can be inferred that alkanes could have played an important role in the bioreduction and capping/stabilization of the gold nanoparticles.

1.4 Conclusions

Bioinspired gold nanoparticle (GNP) synthesis using the obnoxious invasive weed lantana (*Lantana camara*) has been accomplished. It has been demonstrated that extracts from all the parts of the plant – the leaf, the stem and the root – are equally proficient in synthesizing GNPs of different morphology and size. The shapes and sizes of the GNPs observed to depend on the plant part used for the preparation of the extract and the extract – metal ion stoichiometry. GNPs of spherical, anisotropic triangular, pentagonal, rod and truncated triangular shapes, in different sizes, were obtained. The EDX studies indicate the purity, and the XRD and SAED studies indicate the crystalline nature, of the synthesized GNPs. FT–IR spectral studies reveal that amides, proteins and alkanes were responsible for the reduction and stabilization *cum* capping of the GNPs.

Acknowledgement

The authors thank Pondicherry University for rendering the financial support. We acknowledge the CIF, SAIF of Pondicherry University, IIT Madras; and NEHU for their help in SEM, XRD, FTIR, HRSEM, EDAX and TEM, SAED analysis.

References

1. Abbasi T, Anuradha J and Abbasi S A, Nanotechnology and its potential in revolutionizing the pollution control scenario, *IJPHE*, 2009-10, 2, 5-12 (2009).

2. Kaur R and Pal B, Size and shape dependent attachments of Au nanostructures to TiO_2 for optimum reactivity of Au-TiO_2 photocatalysis, *J. Mol. Cat. A: Chem.*, 355, 39-43 (2012).

3. Li Y, Liu X and Lin Z, Recent developments and applications of surface plasmon resonance biosensors for the detection of mycotoxins in foodstuffs, *Food Chem*, 132, 1549-1554 (2012).

4. She H, Chen Y, Chen X, Zhang K, Wang Z and Peng D L, Structure, optical and magnetic properties of Ni@Au and Au@Ni nanoparticles synthesized via non-aqueous approaches, *J Mat. Chem*, 22, 2757-2765 (2012).

5. Jain S, Hirst D G and O'sullivan J M, Gold nanoparticles as novel agents for cancer therapy, *The British J Radiology*, 85, 101-113 (2012).

6. Abbasi S A, Abbasi T and Anuradha J, A process for synthesis of metal nanoparticles from aquatic weeds, Offl. J. Patent Off, dt: 20.04.2012, 6184 (2012).

7. Anuradha J, Abbasi T and Abbasi S A, 'Green' synthesis of gold nanoparticles with aqueous extracts of neem (*Azadirachta indica*), *Res J Biotech, 5, 1, 75-79 (2010).*

8. Anuradha J, Abbasi T and Abbasi S A, Biomimetic synthesis of gold nanoparticles using *Aloe vera. Inter J Environ Sci & Engi Res*, 2, 1-5 (2011b).

9. Iravani S, Green synthesis of metal nanoparticles using plants, *Green Chemistry*, 13, 2638–2650 (2011).

10. Sujitha M V and Kannan S, Green synthesis of gold nanoparticles using Citrus fruits (*Citrus limon, Citrus reticulata* and *Citrus sinensis*) aqueous extract and its characterization, *Spectro. Acta Part A: Mol. and Biomol. Spectroscopy*, 102, 15-23 (2013).

11. Abbasi S A, Abbasi T, Anuradha J, Neghi N, Pirathiba S and Ganaie, S U, Gainful utilization of four otherwise worthless and problematic weeds for silver nanoparticle synthesis. Offl J Patent Off dt: 15.07.2011, 11869 (2011).

12. Anuradha J, Abbasi T and Abbasi S A, Facile 'phyto' fabrication of silver nanoparticles of diverse geometries with concomitant utilization of a pernicious terrestrial weed. In: Proceedings of the International conference on Green Technology and Environmental Conservation (GTEC-2011), Sathyabama University, Chennai, IEEE, 216-223 (2011c).

13. Thirumurugan A, Tomy N A, Kumar H P and Prakash P, Biological synthesis of silver nanoparticles by *Lantana camara* leaf extracts. *Inter J Nanomaterials and Biostructures*, 1, 22–24 (2011).

14. Sivakumar P, Nethradevi C and Renganathan S, 2012. Synthesis of silver nanoparticles using *Lantana camara* fruit extract and its effect on pathogens, *Asian J. Pharmaceutical and Clinical Research*, 5, 97-101 (2012).

15. Kumarasamyraja D and Jagannathan N S, Antimicrobial activity of biosynthesized silver nanoparticles prepared from the leaf extract of *Lantana camara*, *Inter. Research J. Pharmacy*, 4, 203-207 (2013).

16. Majumder D R, Bioremediation: Copper nanoparticles from electronic-waste, *Inter. J. Engineering Sci. and Technol*, 4, 4380–4389 (2012).

17. Gooden B, French K and Turner P J, Invasion and management of a woody plant, *Lantana camara* L., alters vegetation diversity within wet sclerophyll forest in southeastern Australia, *Forest Ecology & Management*, 257, 960–967 (2009).

18. Patel S, A weed with multiple utility: *Lantana camara*, *Rev Environ Sci Biotechnol*, 10, 341–351 (2011).

19. Suthar S and Sharma P, Vermicomposting of toxic weed–*Lantana camara* biomass: Chemical and microbial properties changes and assessment of toxicity of end product using seed bioassay. *Ecotoxicology & Environmental Safety*, 95, 179-187 (2013).

20. APHA (American Public Health Association), Standard methods of water and wastewater. 22nd ed. American Public Health Association, American Water Works Association and Water Environment Federation publication. Washington D.C. (USA) (2012).

21. Anuradha J, Abbasi T and Abbasi S A, Rapid and Reproducible 'Green' Synthesis of Silver Nanoparticles of Consistent Shape and Size Using *Azadirachta indica*, *Res J Biotech*, 6, 69-70 (2011a).

22. Mulvaney P, Surface Plasmon Spectroscopy of Nanosized Metal Particles, *Langmuir*, 12, 788–800 (1996).

23. Link S and El-Sayed M A, Optical properties and ultrafast dynamics of metallic nanocrystals, *Annu Rev Phys Chem*, 54, 331-366 (2003).

24. Shankar S S, Rai A, Ahmad A and Sastry M, Controlling the optical properties of lemongrass extract synthesized gold nanotriangles and potential application in infrared-absorbing optical coatings, *Chem Mater*, 17, 566-572 (2005).

25. Liz-Marzan L M, Tailoring surface plasmons through the morphology and assembly of metal nanoparticles, *Langmuir*, 22, 1, 32–41 (2006).

26. Philip D, Biosynthesis of Au, Ag and Au–Ag nanoparticles using edible mushroom extract, *Spectrochimica Acta Part A*, 73, 374- 381 (2009).

27. Shankar S S, Ahmad A, Parsricha R and Sastry M, Bioreduction of chloroaurate ions by geranium leaves and its endophytic fungus yields gold nanoparticles of different shapes. *J Mat Chem*, 13, 1822-1826 (2003).

28. Borchert H, Shevchenko E V, Robert A, Mekis I, Kornowski A, Grubel G and Weller H, Determination of nanocrystal sizes: a comparison of TEM, SAXS, and XRD studies of highly monodisperse $CoPt_3$ particles, *Langmuir*, 21, 1931-1936 (2005).

29. Navaladian S, Viswanathan B, Varadarajan T K and Viswanath RP, A rapid synthesis of oriented palladium nanoparticles by UV irradiation, *Nanoscale Res. Lett, 4,* 181–186 (2008).

30. Khare V, Li Z, Mantion A, Ayi A A, Sonkaria S, Voelkl A, Thunemann A F and Taubert A, Strong anion effects on gold nanoparticle formation in ionic liquids, *J Mater Chem*, 20, 1332–1339 (2010).

31. Elgersma R C, Dijk V M, Dechesne A C, Nostrum V C F, Hennink W E, Rijikers D T and Liskamp R M, Microwave-assisted polymerization for the synthesis of Abeta (16-22) cyclic oligomers and their self-assembly into polymorphous aggregates, *Org Biomol Chem*, 7, 4517-25 (2009).

32. Kumar V, Yadav S C and Yadav S K, *Syzygium cumini* leaf and seed extract mediated biosynthesis of silver nanoparticles and their characterization, *J Chem Tech & Biotech*, 85, 1301-1309 (2010).

33. Punuri J B, Sharma P, Sibyala S, Tamuli R and Bora U, *Piper betle*-mediated green synthesis of biocompatible gold nanoparticles. *Int. Nano Letters*, 2, 18-26 (2012).